Eurographics Symposium on Rendering (2025)
B. Wang and A. Wilkie (Editors)

Supplementary materials: Bidirectional Plateau-Border Scattering Distribution Function for Accurate and Efficient Foam Rendering

R. Li[1,2], X. Liu[3], R. Wang[1], P. Shen[4], L. Liu[1,2], and B. Wang[5]

[1]University of Science and Technology of China, China
[2]Laoshan Laboratory, Qingdao, Shandong, China
[3]Beihang University, China
[4]The University of Hong Kong, China
[5]Nanjing University, China

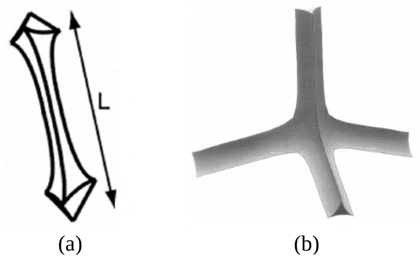

Figure 1: More accurate PB modeling considering (a) a bone-like shape [KHS00] or (b) PB junctions [WP96].

1. Accurate modeling of Plateau borders

In our model, the cross-section of the Plateau border is approximated as three circular arcs. The width of a PB along the axis is fixed as well. A more realistic PB has a bone-like shape [KHS00] as shown in Fig. 1. Besides, no special treatment is applied to the junctions of Plateau borders. Accurate modeling of the foam structure, including the thin films and Plateau borders, can be performed using triangulation-based methods [Bra92]. We leave it for future work.

2. Implementation details

2.1. Foam structure details

The liquid foam model is generated by the power diagram without performing any simulation. To control the bubble density, we employ 3D Poisson disk sampling [Yuk15]. Additionally, the gaps among bubbles are processed, similar to Yan and Wonka [YW13], aiming for matching real-world conditions.

Our PB is modeled using three tangent cylinders. In the foam structure, in addition to the PBs, we introduce two types of film geometries (see Fig. 2): the disk intersected by a polygon, and the sphere intersected by a polyhedron. We implement them procedurally. In the case of the disk intersected by a polygon, we disregard the intersection points that lie outside both the disk and the polygon. For spheres intersected by a polyhedron, we preserve the intersection points on the sphere while lying within the polyhedron. In Tab. 1, we report the number of primitives contained in the foams in each of our scenes.

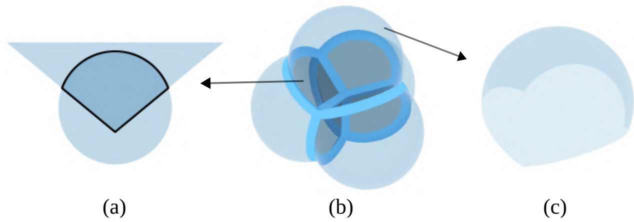

Figure 2: Details of primitives in our foam structure. We have two types of film geometries: a disk cut by a polygon (a) and a sphere cut by a polyhedron. They are derived from the power diagram (b).

Fig.	Primitives
1	1183K
12 (Top)	369K
12 (Bottom)	462K
13	101K
15	285K
17	159K

Table 1: Number of primitives contained within the foams in each scene.

2.2. Network architecture details

We list the encoding functions for some variables in Tab. 2. For outputs of Pos-Net which are used as parameters of Laplace distributions, we provide the decoding for them in Tab. 3.

Parameter	Sampling Function	Encoding
η	$1.3+0.15*\mathcal{U}(0,1)$	$\frac{\eta-1.3}{0.15}$
l'	$10^{-\mathcal{U}(0,2)}$	$-\log_{10}(l')$
α_s	$1-0.5*\mathcal{U}(0,1)^3$	$\sqrt[3]{2-2\alpha_s}$
g	$\mathcal{U}(0,0.95)$	e^g
γ_1	$\mathcal{U}(\frac{2\pi}{3},\pi)$	Frequency encoding
γ_2	$\mathcal{U}(\pi-\gamma_1,\gamma_1)$	Frequency encoding
x_i	$\mathcal{U}(0,1)$	Frequency encoding
z_i	$\mathcal{U}(0,1)$	SH encoding
ϕ_i	$\mathcal{U}(0,2\pi)$	SH encoding

Table 2: Sampling functions and encoding for inputs of our networks. $\mathcal{U}(x,y)$ represents a continuous uniform distribution in $[x,y]$. Note that the encoding of outgoing parameters is the same as incoming parameters, and we do not list them in this table.

Parameter	Pos-Net output	Decoding
$\mu\in\mathbb{R}^3$	$s_1\in\mathbb{R}^3$	$\mathrm{sigmoid}(s_1)$
$\lambda\in\mathbb{R}^3$	$s_2\in\mathbb{R}^3$	e^{s_2}
$a\in\mathbb{R}^3$	$s_3\in\mathbb{R}^3$	e^{s_3}

Table 3: Decoding scheme for Pos-Net outputs.

2.3. Data preparation

The sampling functions we use for generating data are listed in Tab. 2.

3. Accuracy of networks.

In Fig. 3 and Fig. 4, we provide more results to show the accuracy of our three networks on position and direction distributions. The Eval-Net matches the GTs accurately across multiple parameter sets. Pos-Net and Dir-Net are able to approximate the GTs effectively.

References

[Bra92] BRAKKE, KENNETH A. "The Surface Evolver". *Experimental Mathematics* 1.2 (1992), 141–165 1.

[KHS00] KOEHLER, STEPHAN A., HILGENFELDT, SASCHA, and STONE, HOWARD A. "A Generalized View of Foam Drainage: Experiment and Theory". *Langmuir* 16.15 (2000), 6327–6341 1.

[WP96] WEAIRE, D and PHELAN, R. "The physics of foam". *Journal of Physics: Condensed Matter* 8.47 (Nov. 1996), 9519 1.

[Yuk15] YUKSEL, CEM. "Sample Elimination for Generating Poisson Disk Sample Sets". *Computer Graphics Forum (Proceedings of EUROGRAPHICS 2015)* 34.2 (2015), 25–32. ISSN: 0167-7055 1.

[YW13] YAN, DONG-MING and WONKA, PETER. *Gap Processing for Adaptive Maximal Poisson-Disk Sampling*. 2013 1.

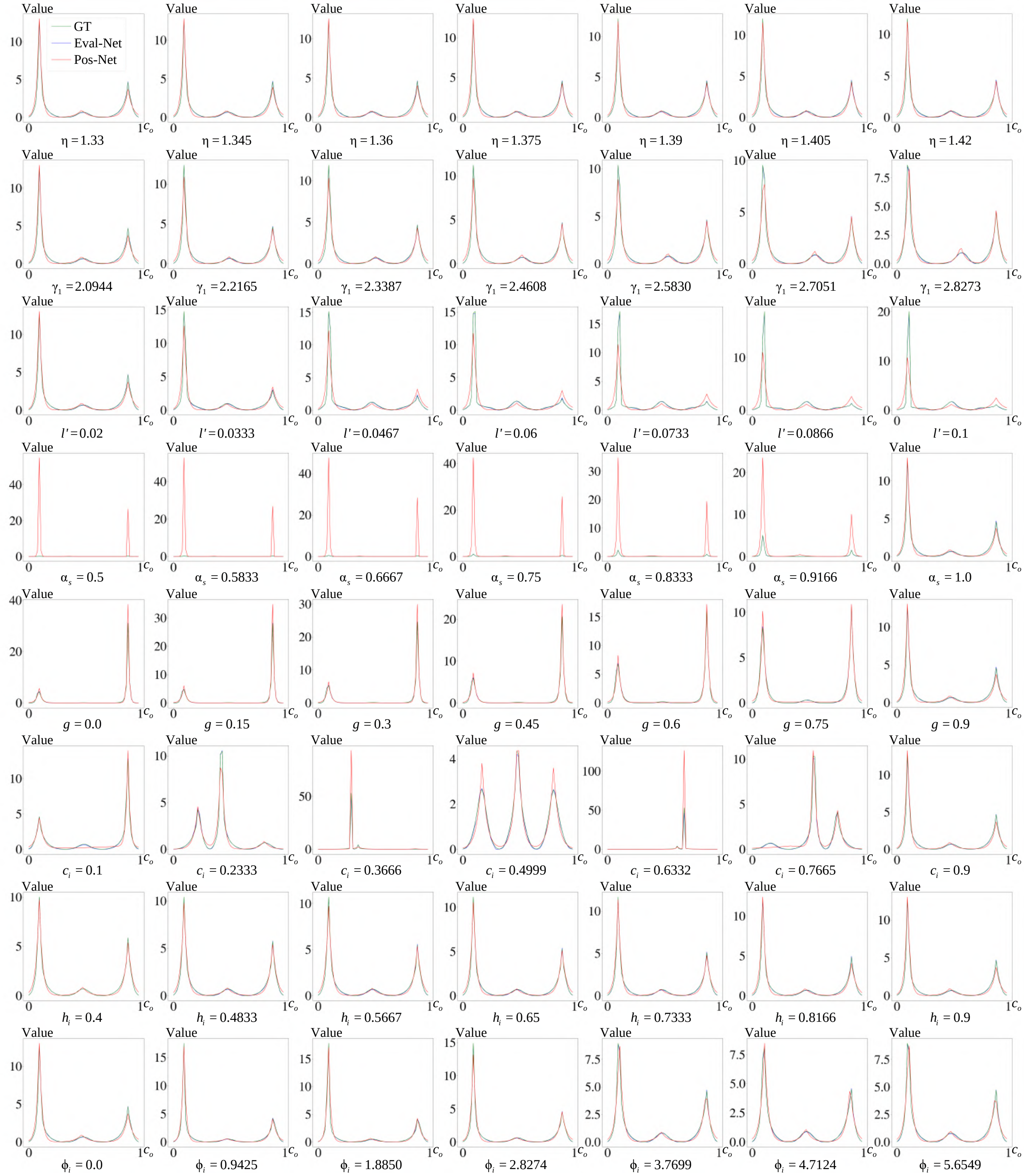

Figure 3: The validation of our Eval-Net and Pos-Net on position distribution. Starting with a set of initial parameters ($\eta = 1.33$, $l' = 0.02$, $\alpha_s = 1$, $g = 0.9$, $\gamma_1 = \frac{2\pi}{3}$, $\gamma_2 = \frac{2\pi}{3}$, $c_i = 0.75$, $h_i = 0.9$, $\phi_i = 3.14$), we show the results in each row by varying one parameter at a time while keeping the others fixed. Eval-Net can approximately match the GT. Pos-Net can closely approximate the position distribution of Eval-Net. Note that when $\alpha_s < 1$, the results of GT and Eval-Net are not normalized, while Pos-Net produces normalized probability distributions.

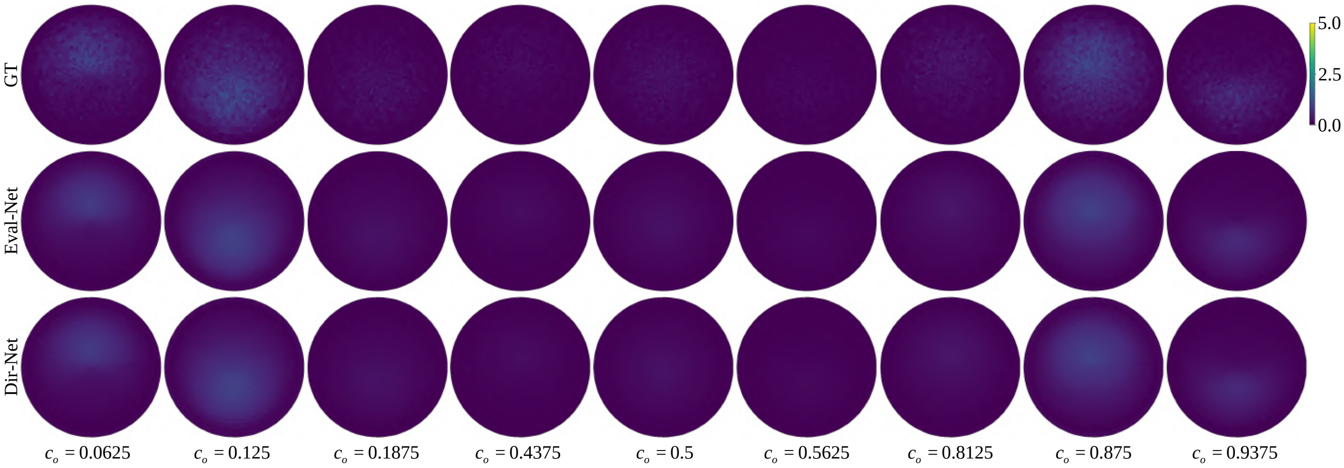

(a) ($\eta = 1.33$, $l' = 0.02$, $\alpha_s = 0.9$, $g = 0.9$, $\gamma_1 = 2.0944$, $\gamma_2 = 2.0944$, $c_i = 0.9$, $h_i = 0.9$, $\phi_i = 0.0$)

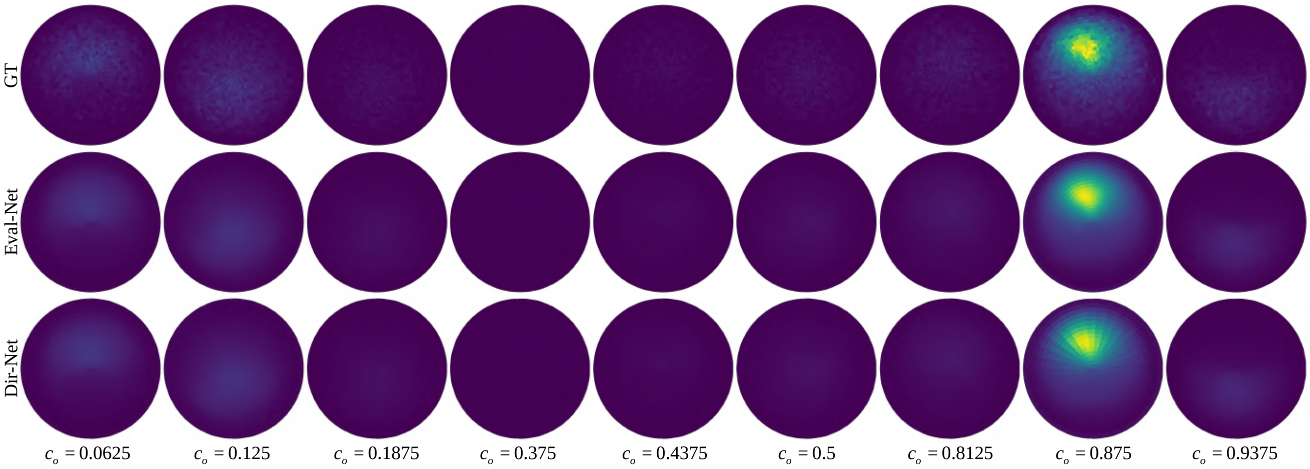

(b) ($\eta = 1.33$, $l' = 0.02$, $\alpha_s = 1.0$, $g = 0.9$, $\gamma_1 = 2.0944$, $\gamma_2 = 2.0944$, $c_i = 0.1$, $h_i = 0.9$, $\phi_i = 0.0$)

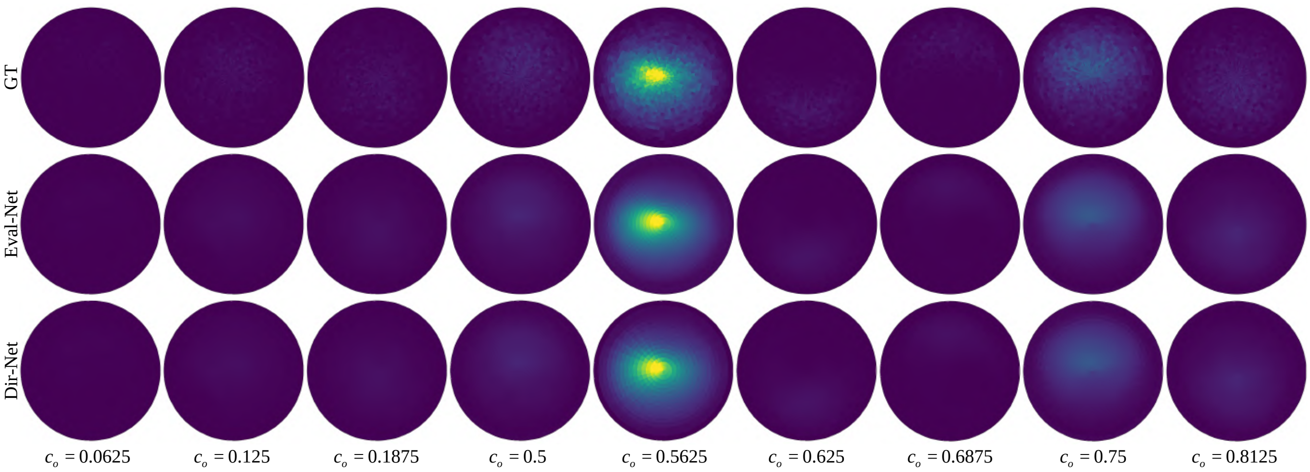

(c) ($\eta = 1.33$, $l' = 0.02$, $\alpha_s = 1.0$, $g = 0.9$, $\gamma_1 = 2.0944$, $\gamma_2 = 2.0944$, $c_i = 0.7$, $h_i = 0.9$, $\phi_i = 0.0$)

Figure 4: The validation of our Eval-Net and Dir-Net on direction distribution. We choose three sets of parameters and show the direction distribution at different c_o. Our Eval-Net approximates the GTs with high accuracy. Our Dir-Net can effectively fit the direction distribution of Eval-Net.